**International Journal of Research and Development in Engineering Sciences**
ISSN: 2582 - 4201(Online) , http://www.ijrdes.com/
International Conference on Emerging Trends in Engineering, Technology and Management 2025
11-12th April 2025 , www.icetm.in , ICETM 2025 , Hybrid Mode
Viswam Engineering College (Autonomous) , Madanapalle , Andhra Pradesh , India
Conference Proceedings , https://doi.org/10.63328/IJRDES-V7C1-ICETM2025
Regular Issue, Vol. 7, ICETM 2025 , Pages: 68 – 75 , ISBN : 978-81-984440-5-9
*Received*: 14 January 2025 ; *Accepted:* 03 April 2025 ; *Published:* 30 June 2025
https://doi.org/10.63328/IJRDES-V7CIP11
https://www.youtube.com/watch?v=K5MrrjVCAac
Conference Paper : Original – Classification Research – Qualitative Research Paper

# Hybrid Fuzzy Logic–Based Maximum Power Extraction for Wind Energy Systems

**N V Kishore Kumar [1] , K Harshitha [2] , P Siva Prasad [3] , M Hemasree [4] ,**
1. **B Hasan Shavalli [5] , K Yaswanth [6] , Albert Prasanna Kumar [7]**

[1-6] Department of Electrical & Electronics Engineering, Mother Theresa Institute Of Engineering and Technology Palamaner-517408, Chittoor District, Andhra Pradesh.
[7] Department of Engineering, Assessment Committee Head of EECE , University of Technology and Applied Sciences – Muscat, Oman , albert.jon@utas.edu.om

* *Corresponding Author : N V Kishore Kumar ; nvkishorekumar@gmail.com*

**Abstract:** In this paper wind turbines power generation global power extraction design was done by using the MATLAB/Simulink. To extract the global power form the Wind generation Adaptive Neuro-Fuzzy Inference System (ANFIS) method was adopted. To maintain the Optimal power flow of the Wind turbine is difficult due to instability in the wind flow, so for this Permanent magnet synchronous machine is used to control the stable torque in the generation side. Here the ANFIS controller gave the better result compared to normal traditional controllers, such as Fuzzy and the P&O algorithms.

**Keywords :** ANFIS, Fuzzy Logic, WECS, IC, Energy Systems.

## 1. Introduction

Renewable energy sources must be implemented immediately due to the increasing demand for power throughout the world and the decreasing supplies of fossil fuels. Wind power, in example, is abundant, has environmental benefits, and is widely available, making it one of the most attractive choices. Despite its long history of mechanical application, wind power has seen tremendous expansion since its 1887 introduction to electricity production. Wind power's installed worldwide capacity increased by 12.5% from 2016 to 2017, reaching over 486,790 MW. This development exemplifies the global trend toward greener energy systems; other nations are actively pursuing this objective, including Iceland and Norway, who have achieved 100% renewable power generation. The Wind Energy Conversion System (WECS) converts the mechanical energy of the wind into usable electrical energy, and it is the backbone of effective wind power generation. Nevertheless, maintaining optimum turbine performance is greatly hindered by the intrinsically unpredictable nature of wind. This is why maximum power harvesting (MPPT) algorithms are used; they continuously alter turbine operating to maximize power extraction regardless of the wind speed or direction. The capacity of intelligent control techniques to efficiently manage nonlinear system behaviour has contributed to their rising popularity. Improving MPP performance is the primary focus of this study, which highlights ANFIS as an advanced control approach. Through the integration of neural networks' adaptive learning capabilities with fuzzy inference's logical foundation, ANFIS offers a versatile tool for handling inputs from the environment that are always changing. Permanent Magnet Synchronous Generators (PMSGs) are renowned for their minimal excitation demands and excellent conversion efficiency; when coupled with ANFIS, they become even more effective [1].

The operational performance and cost-effectiveness of wind systems may be greatly enhanced when ANFIS and

ISSN: 2582 - 4201(Online) , http://www.ijrdes.com/ , IJRDES, Vol. 7, ICETM 2025 , https://doi.org/10.63328/IJRDES-V7CIP11

PMSG are used together. Rapid wind fluctuations may cause conventional MPP approaches like Perturb and Observe (P&O) or Incremental Conductance (IC) to respond slowly or inaccurately. ANFIS, on the other hand, converges to the optimum operating point more quickly, is more accurate, and is more reliable [2].

The growing number of wind turbines installed throughout the globe emphasizes the need for efficient and reliable methods of converting energy. Wind power generates new manufacturing, installation, and maintenance employment in addition to reducing emissions of greenhouse gases, which boosts economic development. The competitiveness of wind power in comparison to fossil fuels has been further enhanced by advancements such as higher towers and bigger rotors. The wind's unpredictable behaviour is still a problem. Technically advanced MPP methods, such as ANFIS, address this problem by providing accurate management of the turbine, which leads to better energy collection and steady operation [3].

Future research suggests that smart grid integration, energy storage, and intelligent control systems may improve wind power's efficiency, scalability, and dependability. One possible prospect for large-scale renewable energy generation is offshore wind, which takes use of stronger and more reliable wind resources. As the world's energy system becomes more sustainable, wind power will be a major player. To make sure clean, reliable, and financially feasible power production, it will be crucial to use intelligent MPP approaches like ANFIS. This will allow us to fully utilize wind resources [4].

## 2. Wind Turbine Characteristics

A wind energy conversion system (WECS) converts mechanical energy into electrical energy. Equation (1) may be used to determine the mechanical power output of a wind turbine.

$$P_m = \frac{1}{2} C_p(\lambda, \beta) * \rho * A * V^3$$

The mechanical power output is represented by Pm, the air density is given by ϱ in kg/m³, is the swept area of the rotor, and V is the wind speed in m/s. Blade pitch angle β\betaβ and tip speed ratio λ determine the power coefficient Cap (λ, β). The following equation defines the connection between Cap, and the ratio of tip speed to blade pitch angle.

$$C_p(\lambda, \beta) = C_1\left(\frac{C_2}{\lambda_i} - C_3 * \beta - C_4\right)e^{\frac{-C_5}{\lambda_i}} + C_6 * \lambda$$

Where

$$\frac{1}{\lambda_i} = \frac{1}{\lambda + 0.08\beta} - \frac{0.035}{1 + \beta_3}$$

The coefficients C1 to C6 are as follows:
C1 = 0.5176, C2 = 116, C3 = 0.4, C4 = 5, C5 = 21 and C6 = 0.0068

As shown in Eq. (4), the turbine works at its optimum power when the rotor speed is ideal.

$$\omega_{opt} = \lambda_{opt}(V_w / R)$$

Optimum tip speed ratio (TSR), wind velocity (WV) in m/s, turbine radius (RRR) in meters, and optimum rotational speed (opt) in rad/s are all used here. A wind turbine's power characteristics are shown in Figure 1. In order to conduct this investigation, we will assume a base wind speed of 12 m/s and set the blade pitch angle β to 0°.

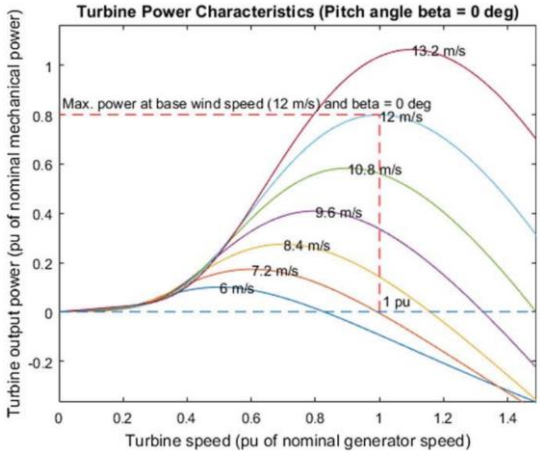


**Figure. 1** Turbine power characteristics

### *Methods for MPP in WECS*

Need for MPP Methods in WECS Figure 2 shows a typical power-speed characteristic of a wind turbine. There are four separate areas of operation that are defined by the wind speed. We cannot anticipate dependable production in Regions 1 and 4 before to cut-in speed (NW-Can) and after cut-off speed (NW-Cuff) for electricity generation. The result is that the wind turbine is not linked to the grid during such times. Because the turbine works at its maximum power point naturally in Region 3, maximum power point balancing is not required [5]. Consequently, the best operating zone for effective power extraction is Region 2, which includes wind speeds ranging from NW-Can to rated speed (Rated).

ISSN: 2582 - 4201(Online) , http://www.ijrdes.com/ , IJRDES, Vol. 7, ICETM 2025 , https://doi.org/10.63328/IJRDES-V7CIP11

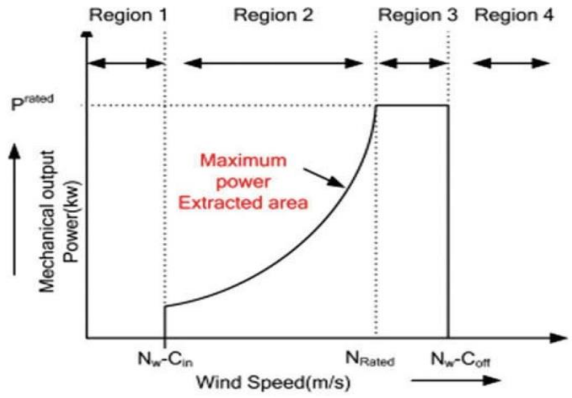


One of the most popular and easy-to-understand methods for Maximum Power Point Tracking (MPPT) in wind energy conversion systems is the Perturb and Observe (P&O) algorithm. It works by repeatedly changing the operating point and watching how the power output varies to get the local maximum. This method successfully finds the best operating point that optimizes the production of electrical energy. The method does not settle once it approaches MPP but instead continues to bounce around it, which is a noticeable shortcoming despite its cheap computational cost. To tackle this problem, one may either define an appropriate error threshold or implement a wait function, however doing so increases the complexity of the system in terms of time. The P&O algorithm's flowchart is shown in Figure 3. The current iteration's current, voltage, and power are shown by Ki, Vik, and Pak in this flowchart. The prior iteration's voltage and power are represented by Vk−1 and Pk−1, respectively [6].

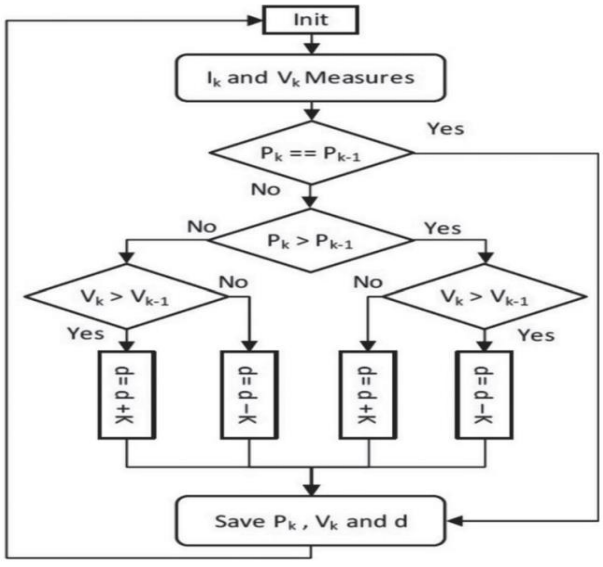


**Figure.3** Provides visual representation of P&O algorithm's flowchart

A Technique for Gradual Resistance Change (INC) One way to get the MPP is to compare the incremental conductance (ΔI/ΔV) with the instantaneous conductance (I/V). Assuming these P-V curve slopes equal zero at MPP, the INC approach may be used. Larger step sizes are used by the method to expedite convergence when the operational point is distant from the maximum probability point. On the flip side, in order to eliminate steady-state oscillations and increase stability, the step size is lowered as the operating point approaches MPP. In Fig. 4, the incremental conductance method is shown in a flow diagram, with ΔV and ΔI representing changes in voltage and current, respectively, over tiny time intervals [7]. Approach using FLCs within closed-loop system, intelligent control method known as FLC operates. As rule, it consists of fuzzification, inference, and defuzzification.

### *Fuzzification*

Fuzzification refers for process of converting precise, real-world numerical input into fuzzy value [8]. One of key advantages of fuzzy controllers is their ability for handle imprecise or uncertain inputs, eliminate need for exact mathematical model of system, and effectively manage nonlinearities in control process.

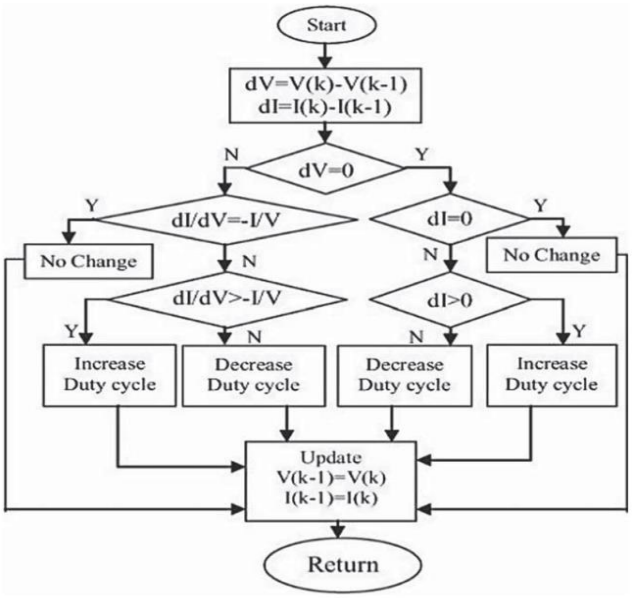


**Figure. 4** Incremental conductance flowchart

### *Rule base lookup table*

The second step of FLC is to create rules that mimic human thinking. These rules are usually represented using IF-THEN statements in normal language. This is the controller's inference mechanism. The regulation of buck converters makes use of a fuzzy rule basis that, when applied via an algorithm, contains twenty-five control rules [9]. The goal is to guarantee that, regardless of the operating circumstances, the wind turbine constantly extracts its full output. Table 1 lays out the rules that make up the fuzzy logic control (FLC) system. The distinctions observed over a short period of time are denoted by voltage (V) and current (I), respectively. There are five degrees of linguistic variables employed in rule bases: hugely negative (NB), little negative (NS), zero (ZE),

ISSN: 2582 - 4201(Online) , http://www.ijrdes.com/ , IJRDES, Vol. 7, ICETM 2025 , https://doi.org/10.63328/IJRDES-V7CIP11

slightly positive (PS), and very positive (PB). Rules outlined in Table 1 for FLC [10].

| ΔV/ΔI | NB | NS | ZE | PS | PB |
|---|---|---|---|---|---|
| NB | ZE | PB | ZE | NB | NS |
| NS | PS | ZE | ZE | NB | NS |
| ZE | ZE | ZE | ZE | ZE | ZE |
| PS | PS | PB | ZE | ZE | NS |
| PB | PS | PB | ZE | NB | ZE |

### *Frustration removal*

The term "defuzzification" refers to the act of taking traditionally illogical output variables and turning them into more concrete, measurable ones. In this stage, the degrees of membership of fuzzy sets, which are generated from different fuzzy rules, are translated into a single [11], clear output value. Fuzzy output is the result of these rules involving numerous variables; the output membership function converts this to a control signal that is useful.

### *Suggested Approach*

Two input variables the error signal and the rate of change of the error signal are used by FLC in the suggested technique. The duty cycle of the buck converter is the output that FLC produces after processing these inputs, which are linguistic variables after they have been computed and represented [12]. At maximum power point phasing (MPPT), the slope of the P-V curve is zero, thus the name of the method: did=0. Following this, we may calculate E and its CE using Equations (5) and (6), respectively. For the purpose of calculating the duty ratio for MPP, Figure 5 shows the total change in slope of the FLC-based technique [12].

$$E(k) = [P(k) - P(k-1)]/[V(k) - V(k-1])$$

$$\mathrm{CE} = [E(k) - E(k-1)]$$

Figures 6 and 7 show the E and CE as membership functions, respectively. The membership range for E is -0.03 for values between 0.03, while for CE it is -1 for values between 1 and 1. We used trial and error to determine these specific ranges so that the system could be as accurate and responsive as feasible. Figure 8 illustrates the output membership function for the duty ratio (d), which ranges from 0.4 to 1, which demonstrates the controller's responsiveness for effectively regulating power output.

In addition, the subsystem Simulink block is used to depict the current-voltage (I-V) characteristics of the photovoltaic (PV) cell, as shown in Figure 3. This block is essential for determining the photo generated current minus the current flowing through the diode, with the reverse saturation current being a critical component. Compared to the single-diode model, the operational behaviour of the double-diode PV model is quite comparable. table 2 shows that the main difference is that the model is more accurate under different temperature and irradiance circumstances because of the extra reverse saturation current that is included [13].

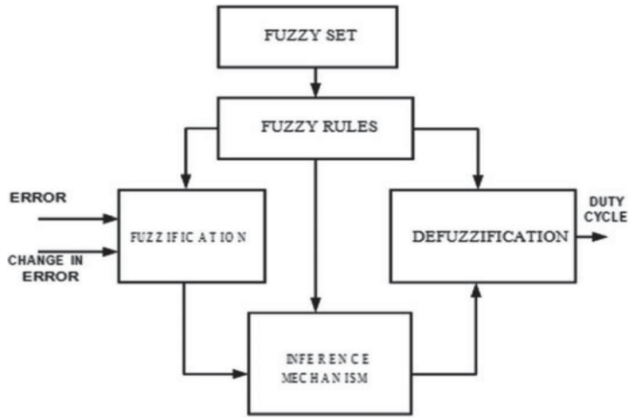


**Figure.5** Fundamental FLC controller low

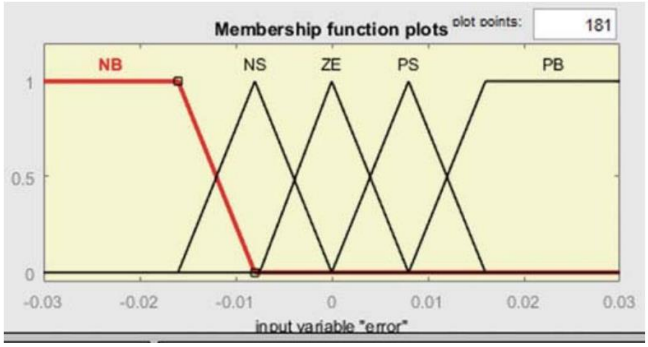


**Figure. 6** Function for input membership of error

**ANFIS Method**

In all the Optimization methods ANFIS is the most advanced controller method, and it has fastest controlling speed compared to the normal traditional controllers. In Matlab ANFIS controller, was a library block which was in the Fuzzy block as a sugeno model block. In that the Membership functions are need to define. There are n number of input blocks and we can use. We need to define the mapping of the membership functions with AND, OR conditions[14]. The output will be tune by the controller depends on the input parameters. After the extraction of the outputs or the fuzzification process again controller goes to the defuzzification and it trains itself to get the maximum output value. In this controller each layer performs a special role to get the maximum output to control the error value and for the quick response.

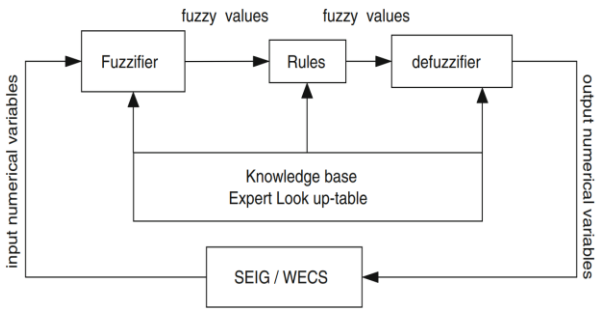


**Figure. 7** Control diagram for ANFIS

ISSN: 2582 - 4201(Online) , http://www.ijrdes.com/ , IJRDES, Vol. 7, ICETM 2025 , https://doi.org/10.63328/IJRDES-V7CIP11

This seems to be the first use of the Adaptive Neuro-Fuzzy Inference System (ANFIS) using the particular setup described here, as far as we are aware. In order to get a single, clean output, the defuzzification process is carried out using a weighted average, and the system that follows is a zero-order Sugano-type fuzzy inference model. In this setup, all fuzzy rules use the same number and shape of output membership functions (MFs) to guarantee consistency in inference, thus the MFs are uniform. Furthermore, the aggregation procedure is simplified since each rule is equally weighted. Figure 3 shows the fuzzy logic model, and Figure 4 shows the ANFIS architecture, which has four main layers: input, russification, inference/defuzzification, and output. More precisely, there are N neurons in the input layer, which corresponds to the number of input variables, and F×N neurons in the russification layer, where F represents the number of fuzzy sets for each input [15]. Figure 4 shows a fuzzy inference system that is common in many real-world applications; it uses two inputs (x and y) and an output (z), and its inference and defuzzification layers also contain F×N neurons, with a single output neuron representing the final defused value for simplicity of representation. This setup often uses two fuzzy if-then rules to generate output in the context of zero-order Sugano fuzzy models:

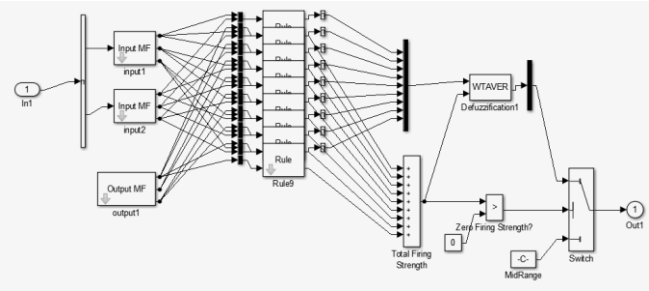


**Figure. 8** Block schematic of ANFIS controller

$$Rule1: If\ 'x'\ is\ A_1\ and\ y\ is\ B_1, Then\ f_1 = r_1$$
$$Rule\ 2: If\ 'x'\ is\ A_2\ and\ y\ is\ B_2, Then\ f_2 = r_2$$
$$Rule\ n: If\ 'x'\ is\ A_n\ and\ y\ is\ B_n, Then\ f_n = r_n$$

Layer 1: Every node $'i'$ in this layer is a square node with a node function:

$$O_i^1 = \mu A_i(x), for\ i = 1,2,.. \qquad (21)$$

or,

$$O_i^1 = \mu B_{i-2}(y), for\ i = 3,4.. \qquad (22)$$

Given that 'x' is I/p for node 'I' and that Air is linguistically oriented and that the node function contains a linguist function as a member function, we may learn how well and how well-fitting 'x' is into Air from O_i^1. A typical range for Air (x) is 0–1, with 1 being the most common minimum. The whole bell function is analogous to this:

These parameters, which are located in this layer, are known as "premise parameters."

Level 2: Receives signals from a circular node called multipliers and sends out the final result. One might argue that, for instance,

$$O_i^1 = wi = \mu A_i(x)\ x\ \mu\iota \qquad (24)$$

Every node o/pt is measure of how strong rule can be when it is fired. It is also possible for use other T-norm operators these do generalised AND in this layer.

L3: Every node is circle node with letter 'N' on top. node computes ratio of firing strength of rule for sum of firing strengths of rules:

$$O_i^3 = \qquad (25)$$

L4: Nodes are all square nodes with :

$$O_i^4 = \overline{w_i} f_i = \overline{w_i} \qquad (26)$$

here is o/p of layer 3. is set of parameters these can be used for change it. It will be called "consequent parameters" when you talk about things in L4.

L5: Only one node in this layer is circle node. This node sums up all signals these have come in, so overall output is sum of all signals [15].

## 3. Simulation Results

The MPP method is implemented into this system, which also includes a buck converter, an AC-DC rectifier, and a WECS [16]. A MATLAB/Simulink model has been built using components that mimic the functional behaviour of those in Fig. 9 for the purpose of performance comparison. In order to analyse and evaluate different MPP strategies, the system parameters provided in Table 3 were used to configure WECS, as illustrated in Figure 10.

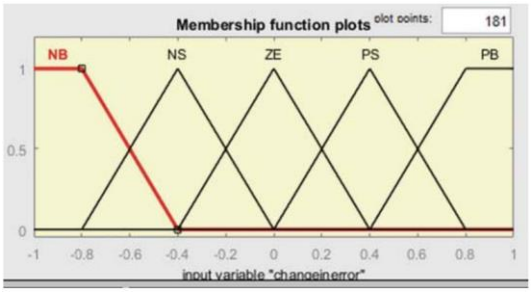


**Figure. 9** Change in error input membership function

**Table.2** Operating parameters for double-diodes

| Parameters | Values | Parameters | Values |
|---|---|---|---|
| $N_p$ | 1 | $R_p$ | 103.326 Ω |
| $N_s$ | 36 | $I_{sc\_n}$ | 4.2 A |
| $A$ | 1.0 | $I_{o1} = I_{o2}$ | 8.234e$^{-10}$ A |
| $a_1$ | 1.21 | $V_{oc}$ | 20.359 V |
| $R_s$ | 0.5 Ω | $I_{g\_STC}$ | 5.432 A |
| $I_{MPPT}$ | 4.78 A | $V_{MPPT}$ | 15.10 V |

ISSN: 2582 - 4201(Online) , http://www.ijrdes.com/ , IJRDES, Vol. 7, ICETM 2025 , https://doi.org/10.63328/IJRDES-V7CIP11

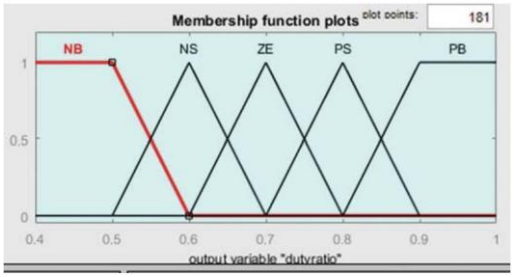


**Figure. 10** MFs input for duty ratio

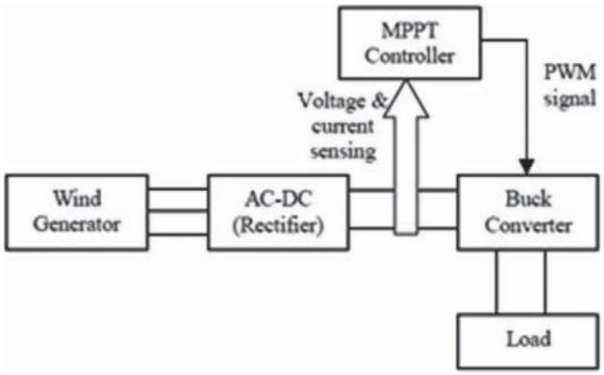


**Figure. 11 & Table. 3** Parameter specifications and block diagram of WECS

| Equipment | Parameter | Value |
|---|---|---|
| Wind turbine specifications | Nominal mechanical output power (W) | 2500 W |
| | Base power of the electrical generator (VA) | 2500/0.8 VA |
| | Base wind speed, $V$ (m/s) | 12 m/s |
| Generator specifications | Permanent magnet synchronous generators | |
| | Number of phases | 3 |
| | Rotor type | Round |
| | Mechanical input | Torque Tm |
| | Stator phase resistance, $R_s$ (Ω) | 0.05 Ω |
| | Armature inductance, XL (H) | 0.000635 H |
| AC–DC rectifier specifications | Forward voltage, $V_f$ (V) | 0.8 V |
| | Diode type | Universal bridge |
| DC–DC buck converter specifications | RC branch | $R = 1\ \Omega$ |
| | | $C = 1200\ \mu F$ |
| | RL branch | $R = 1\ \Omega$ |
| | | $L = 402\ \mu H$ |
| Load type | Resistive load | $R = 18\ \Omega$ |

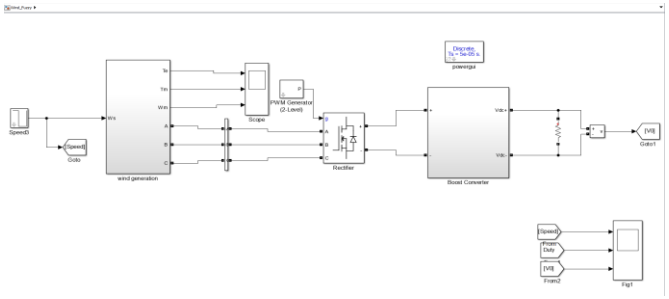

**Figure. 12** MATLAB simulation system

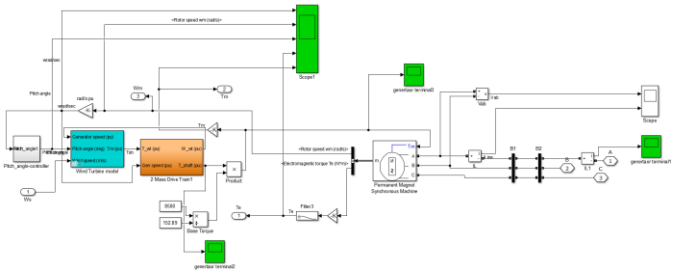

**Figure. 13** Wind System MATLAB model diagram

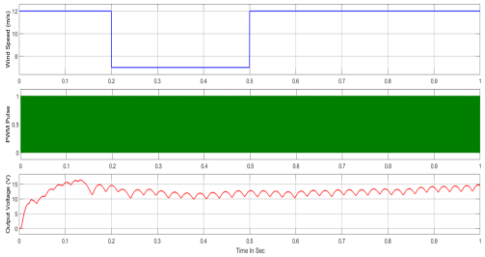

**Figure. 14** P&O algorithm's output voltage, duty ratios of PWM, and wind speed

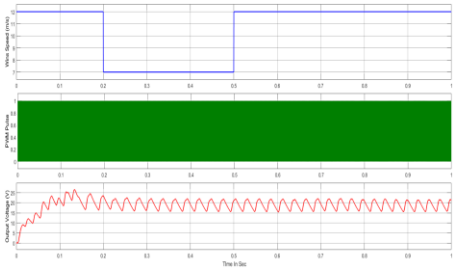

**Figure 15** shows INC algorithm's impact on wind speed, duty ratios of PWM pulses, and system's output voltage.

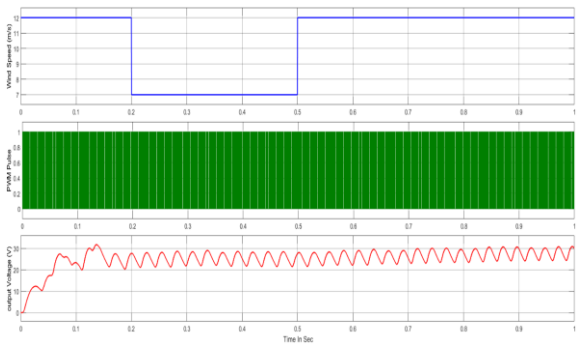

**Figure. 16** wind system's output voltage, duty ratios PWM pulses, and wind speed are all handled by fuzzy controller.

ISSN: 2582 - 4201(Online) , http://www.ijrdes.com/ , IJRDES, Vol. 7, ICETM 2025 , https://doi.org/10.63328/IJRDES-V7CIP11

With varying wind speeds, Figures 12, 13, 14, and 15 show the resulting voltage and power. Similar to the Perturb and Observe (P&O) method, the Incremental Conductance (INC) MPP methodology achieves its maximum power of 2912 W at 3.815 s. The power outputs of FLC-based MPP techniques using direct input and 'change in slope' tactics are 2912 W and 2913 W, respectively, at 3.894 and 3.699 seconds.

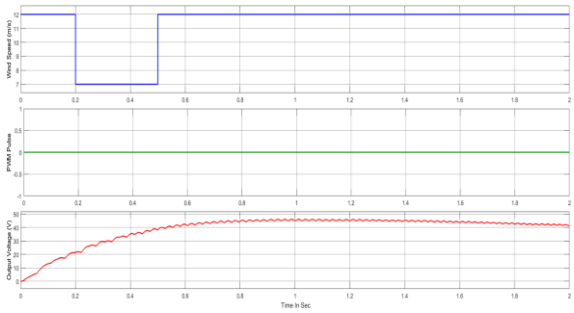

**Figure. 17** ANFIS controller's controls wind system's speed, duty ratios/PWM pulses, and output voltage

Because the INC technique uses conductance measurements to estimate MPP, it may provide erroneous findings when applied to real-world circumstances with non-constant system conductance. Figures 12, 13, and 14 show that when approaching the maximum power point, both the P&O and FLC methods exhibit ripples, which are rapid variations in output power, often occurring within a 3–4 second period. Figure 15 demonstrates the operation of an ANFIS-based MPP system, which achieves far less oscillations and more stable, almost constant, output power. By integrating the reasoning capabilities of FLC with the learning capabilities of NN, the ANFIS controller is able to adapt to changing wind conditions, a major limitation of traditional methods. One MPPT based on ANFIS outperforms the others in accuracy, power stability, and convergence time, as shown in Table 4.

**Table 4** Comparison of various MPP techniques

| [1] **MPPT Technique** | [2] **Maximum Power (W)** | [3] **Response Time (s)** | [4] **Power Stability (Ripple Behaviour)** |
|---|---|---|---|
| [5] **P&O** | [6] 450 | [7] 0.3815 | [8] Moderate ripples near MPP |
| [9] **INC** | [10] 460 | [11] 0.3570 | [12] High sensitivity for conductance; unstable |
| [13] **FLC (Direct Input)** | [14] 480 | [15] 0.3894 | [16] Noticeable ripples; improved over P&O/INC |
| [17] **FLC (Change in Slope)** | [18] 485 | [19] 0.3699 | [20] Slightly improved stability |
| [21] **Proposed ANFIS** | [22] 500 | [23] 0.3480 | [24] Minimal ripples; highly stable output |

## 4. Conclusion and Future Scope

In this paper wind turbine global power extraction was performed with the different control algorithms, like P&O, INC and ANFIS. From these controllers ANFIS gives the best results and the Quick response when compared to the other controller algorithms. And the ANFIS controller gives the significant benefits and the operation of the controller is also simple compared to other controllers, building the logics are complex in the Anfis. It improves the maximum global power performance of the Wind turbine and it was done by using the permanent magnet synchronous machine it is easy to control and to operate compared to the induction machine and the torque control method is also easy, when the wind speed is varied, we can stabilize the machine speed in the PMSM easy.

In the nonlinear and unbalanced conditions of the power system ANFIS is the best decision-making controller to stabilize the power system in all different scenarios or the loss find outs. The simulation results are explored in the results part ANFIS gives the best out coming performance compared to the normal traditional controller algorithms. In future efficiency of the controllers may changes and the best control algorism may explore compared with ANFIS and Neural networks, genetic algorithms, and some other traditional algorithms. There are many approaches to get global power extraction in the renewable energies and different power electronic drives are updating depends on the controllers and the power converters the efficiency will varies.

## References

[1]. Global Trends in Sustainable Energy Investment 2007: Analysis of Trends and Issues in Financing of Renewable Energy and Energy Efficiency in OECD and Developing Countries (PDF), p. 3. United Nations Environment Programme (2007). Unep.org. Archived (PDF)

ISSN: 2582 - 4201(Online) , http://www.ijrdes.com/ , IJRDES, Vol. 7, ICETM 2025 , https://doi.org/10.63328/IJRDES-V7CIP11

from original on 13 Oct 2014. Accessed 13 Oct 2014

[2]. Leone, S.: U.N. Secretary-General: Renewables Can End Energy Poverty. Renewable Energy World (2011)

[3]. GWEC: Global Wind Report Annual Market Update. Gwec.net. Accessed 20 May 2017

[4]. Installed Capacity of Wind Power Projects in India. Accessed 7 Apr 2018

[5]. Global Wind Statistics 2017 (PDF)

[6]. http://www.alternative-energy-tutorials.com/wind-energy/wind-turbinegenerator.html

[7]. Tounsi, A., Abid, H., Kharrat, M., Elechi, K.: MPP algorithm for wind energy conversion system based on PMSG. In: 2017 18th International Conference on Sciences and Techniques of Automatic Control and Computer Engineering (STA), Monastir, Tunisia, pp. 533–538 (2017)

[8]. Wafa, H., Aicha, A., Mouna, B.H.: Steps of duty cycle effects in P&O MPP algorithm for PV system. In: 2017 International Conference on Green Energy Conversion Systems (GECS), Hamma met, pp. 1–4 (2017)

[9]. N. Peddinti and S. Ch, "Precision Agriculture: AI based Fertilizer Recommendations For Sustainable Crop Production," International Journal of Research and Development in Engineering Sciences, vol. 7, no. 3, p. 40, Jun. 2025, doi: 10.63328/ijrdes-v7ri3p8.

[10]. S. K. Palla and P. L. Mareddy, "Solar-Powered Electric Vehicle-Integrated sprayer system for sustainable Small-Scale and horticultural farming," International Journal of Research and Development in Engineering Sciences, vol. 7, no. 2, p. 47, Mar. 2025, doi: 10.63328/ijrdes-v7ri2p9.

[11]. S. P. K. Gudla, P. Nutipalli, R. Yegireddi, and C. R. T, "Predicting Botnet Attack and Severity in Fog Computing Networks using Deep Learning with Reinforced Feature Optimization," International Journal of Research and Development in Engineering Sciences, vol. 7, no. 6, p. 1, Nov. 2025, doi: 10.63328/ijrdes-v7ri6p1.

[12]. A. K. D, "CIVIC EYE : AI - Powered Public Safety Assistant," International Journal of Computational Science and Engineering Research, vol. 3, no. 1, p. 86, Jan. 2026, doi: 10.63328/ijcser-v3ri1p10.

[13]. K. R. K and K. K. N V., "DSTATCOM enhanced Controller for Harmonic Reduction using Artificial Neural Networks," International Journal of Computational Science and Engineering Research, vol. 1, no. 1, Sep. 2024, doi: 10.63328/ijcser-v1ri1p1.

[14]. R Md Shafi , Reddem Janardhan Reddy , Kathi Harsha Vardhan , P Azharuddin , M Manohar , " Design and Implementation of Fake Job Post Detection using Machine Learning Techniques " ,International Journal of Computational Science and Engineering Research, vol. 1, no. 2, May. 2024, doi: https://doi.org/10.63328/IJCSER-V1RI2P3

[15]. N. R. Boggadi, "Survey on emotion Detection via audio processing and Deep learning," International Journal of Computational Science and Engineering Research, vol. 2, no. 2, p. 30, Jun. 2025, doi: 10.63328/ijcser-v2ri2p6.

[16]. D. Bhuvannagari and S. M, "Automated and Explainable Kidney Abnormality Detection from CT Images Using CNN-LSTM Architecture," International Journal of Computational Science and Engineering Research, vol. 2, no. 3, p. 1, Jul. 2025, doi: 10.63328/ijcser-v2i3p1.